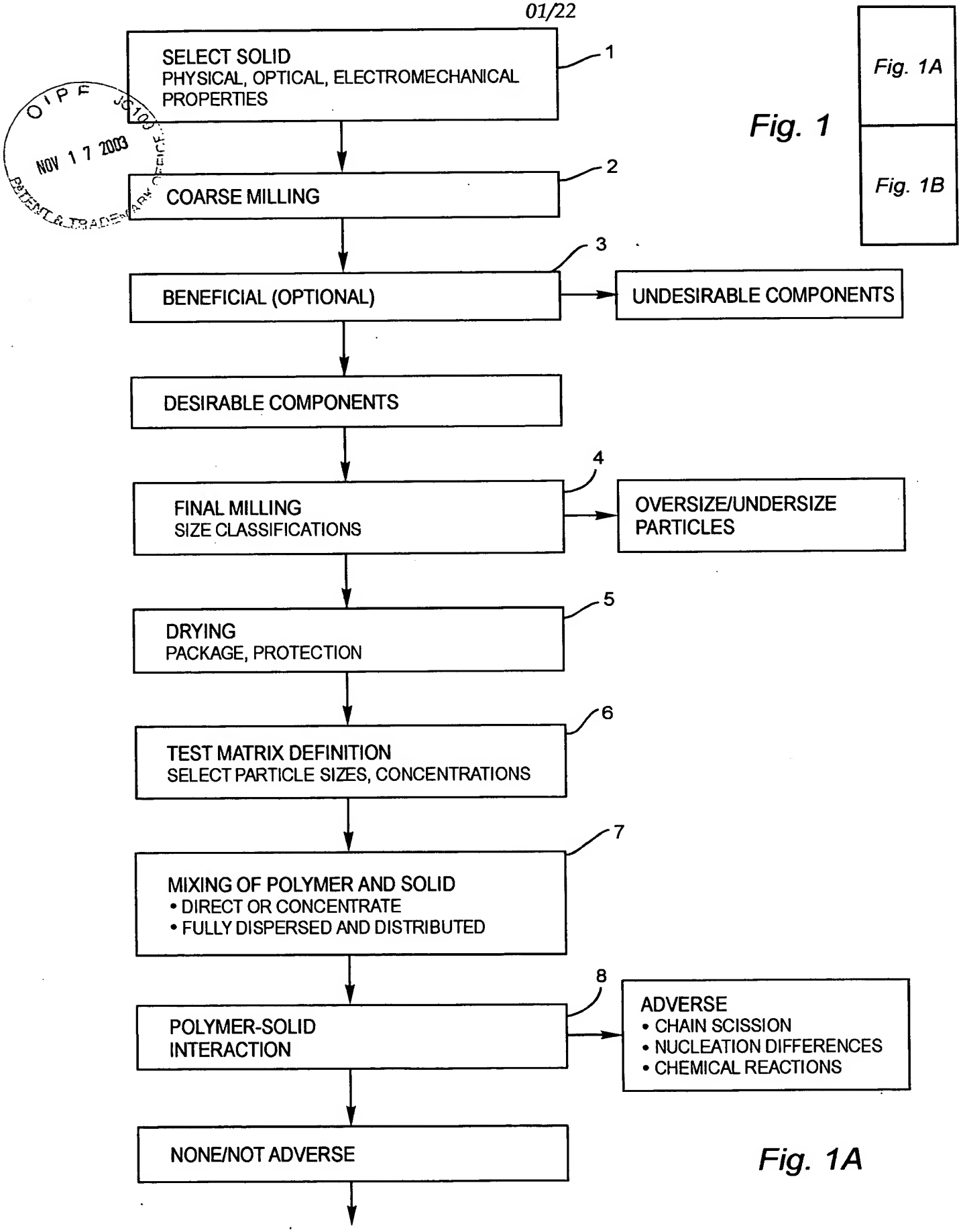

Fig. 1

Fig. 1A

Fig. 1B

Fig. 1A

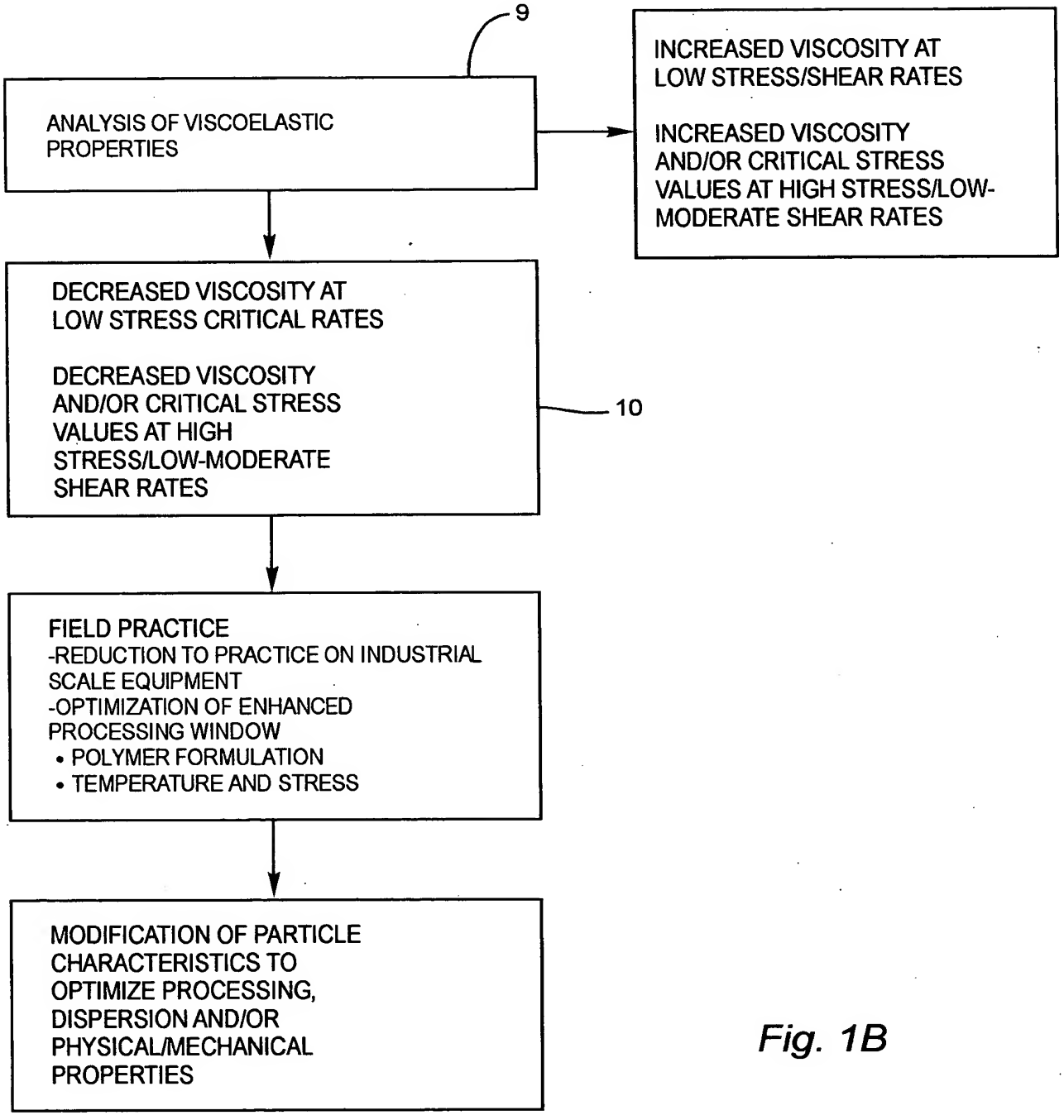

Fig. 1B

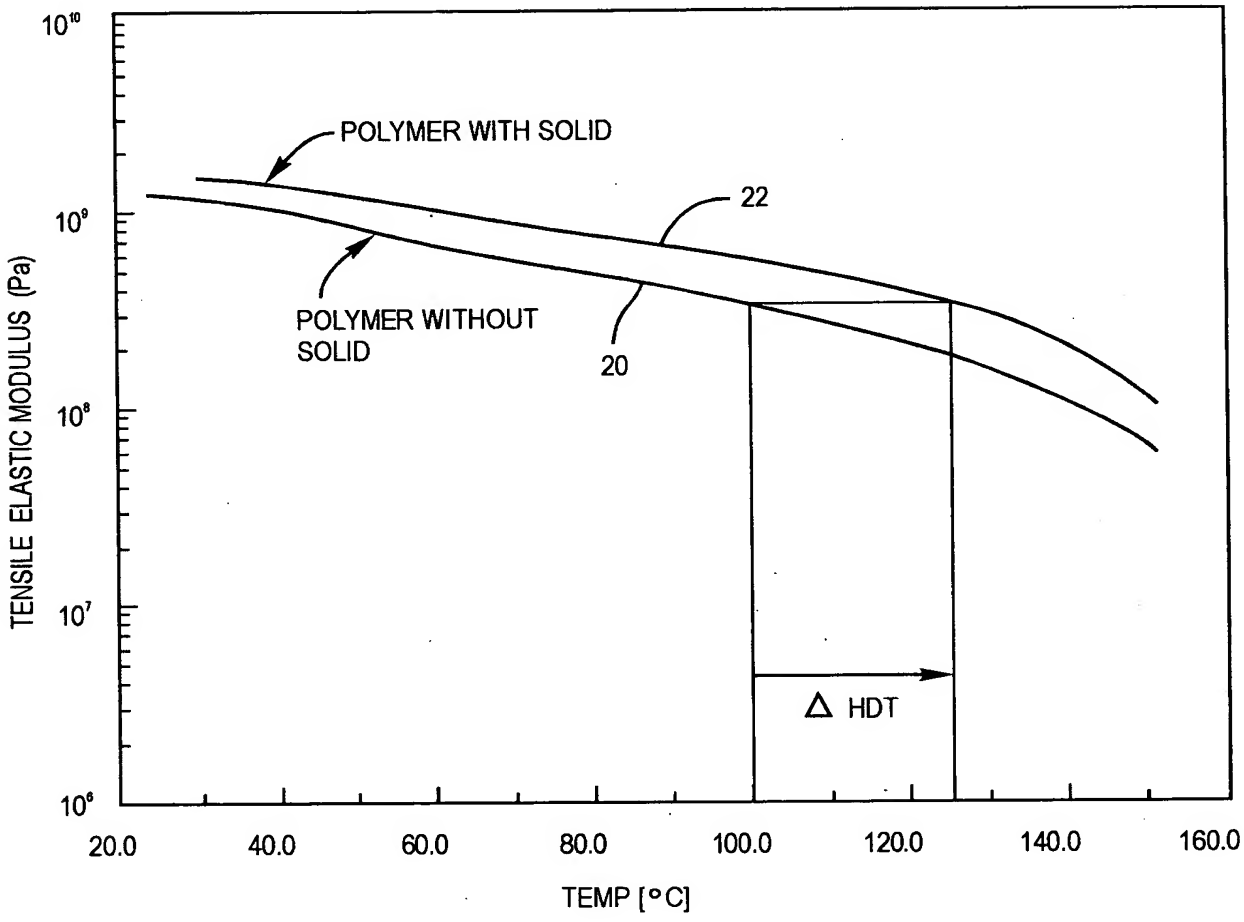

TENSILE ELASTIC MODULUS OF POLYMER AS FUNCTION OF TEMPERATURE

Fig. 2

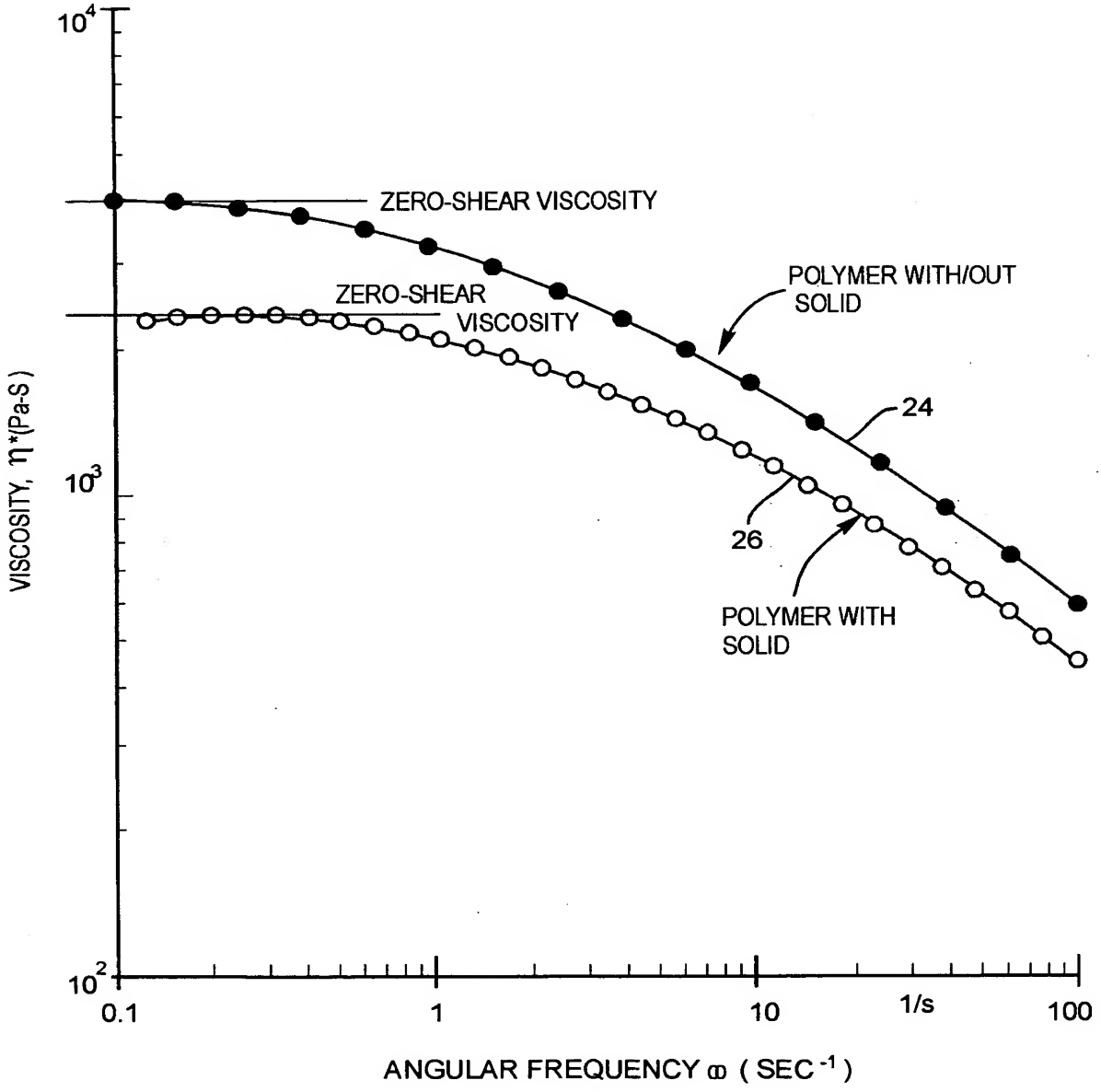

DETERMINATION OF ZERO-SHEAR VISCOSITY FROM VISCOSITY-FREQUENCY PLOT

Fig. 3

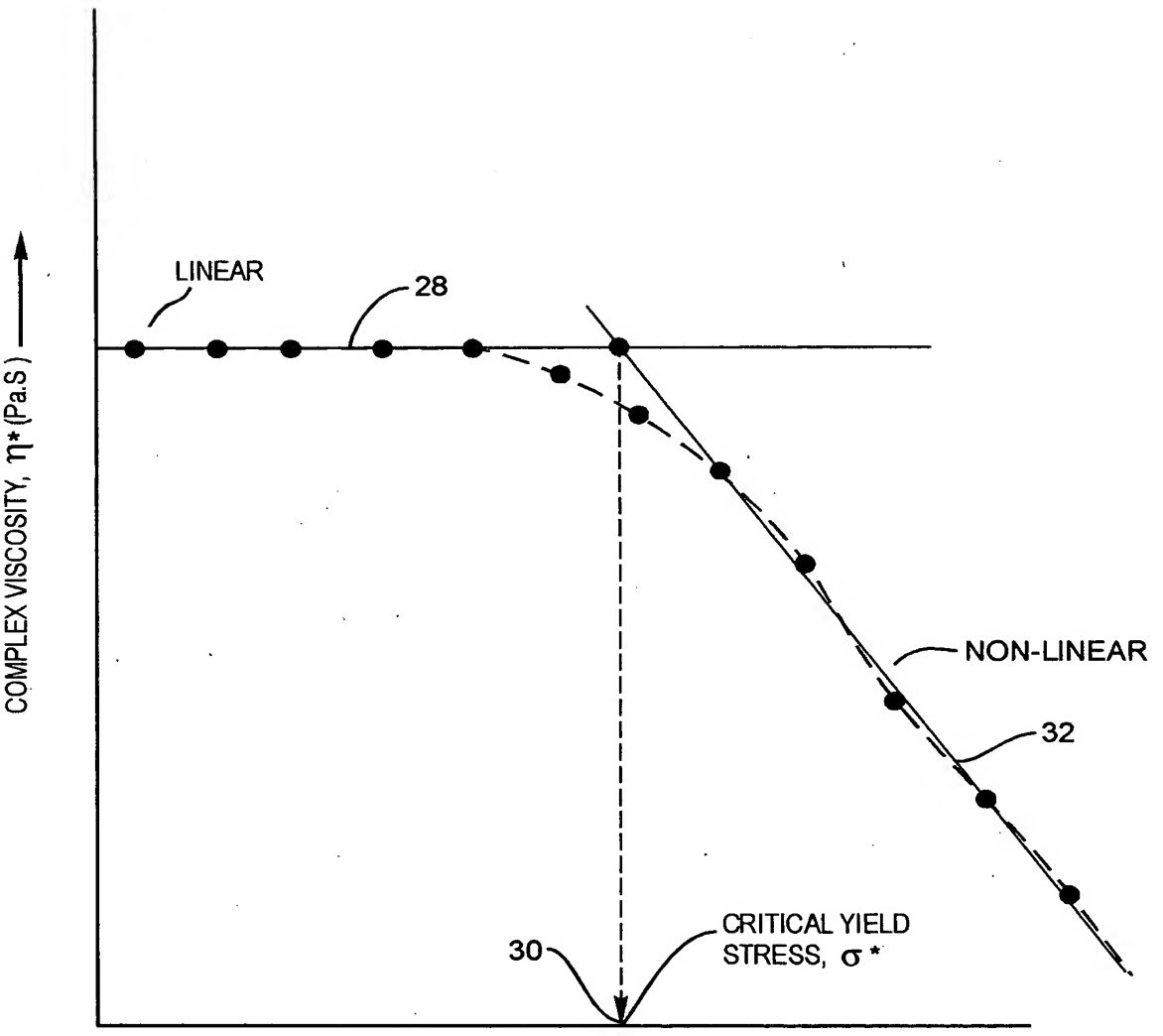

DETERMINATION OF CRITICAL STRESS VALUE FROM VISCOSITY-STRESS CURVES.

Fig. 4

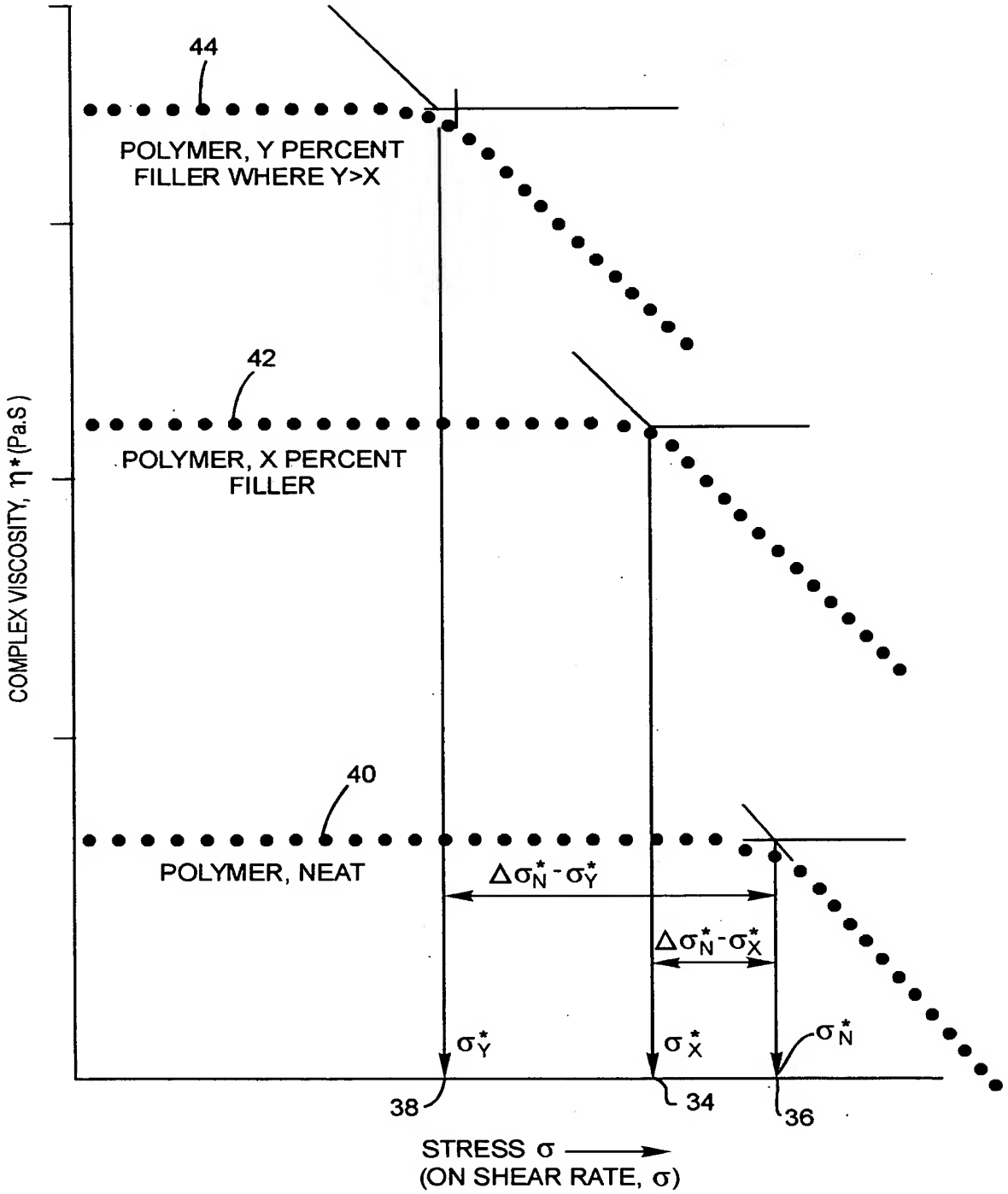

EFFECT OF FILLER, CONCENTRATION ON VISCOSITY AND CRITICAL STRESS VALUE

Fig. 5

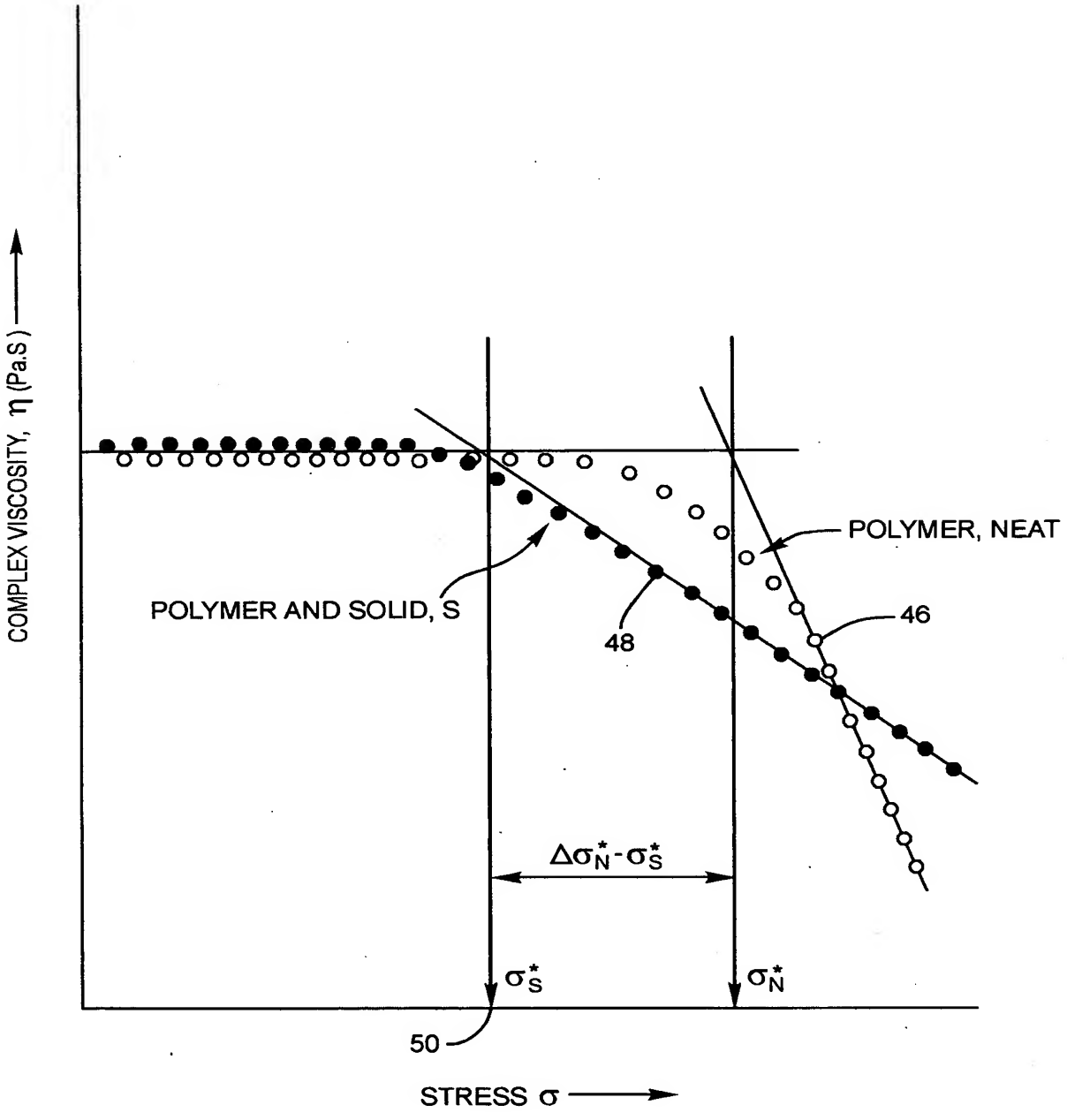

EFFECT ON CRITICAL STRESS VALUE BY ADDING SOLID WITH PREFERRED SIZE RANGE AND CONCENTRATION TO NEAT POLYMER

Fig. 6

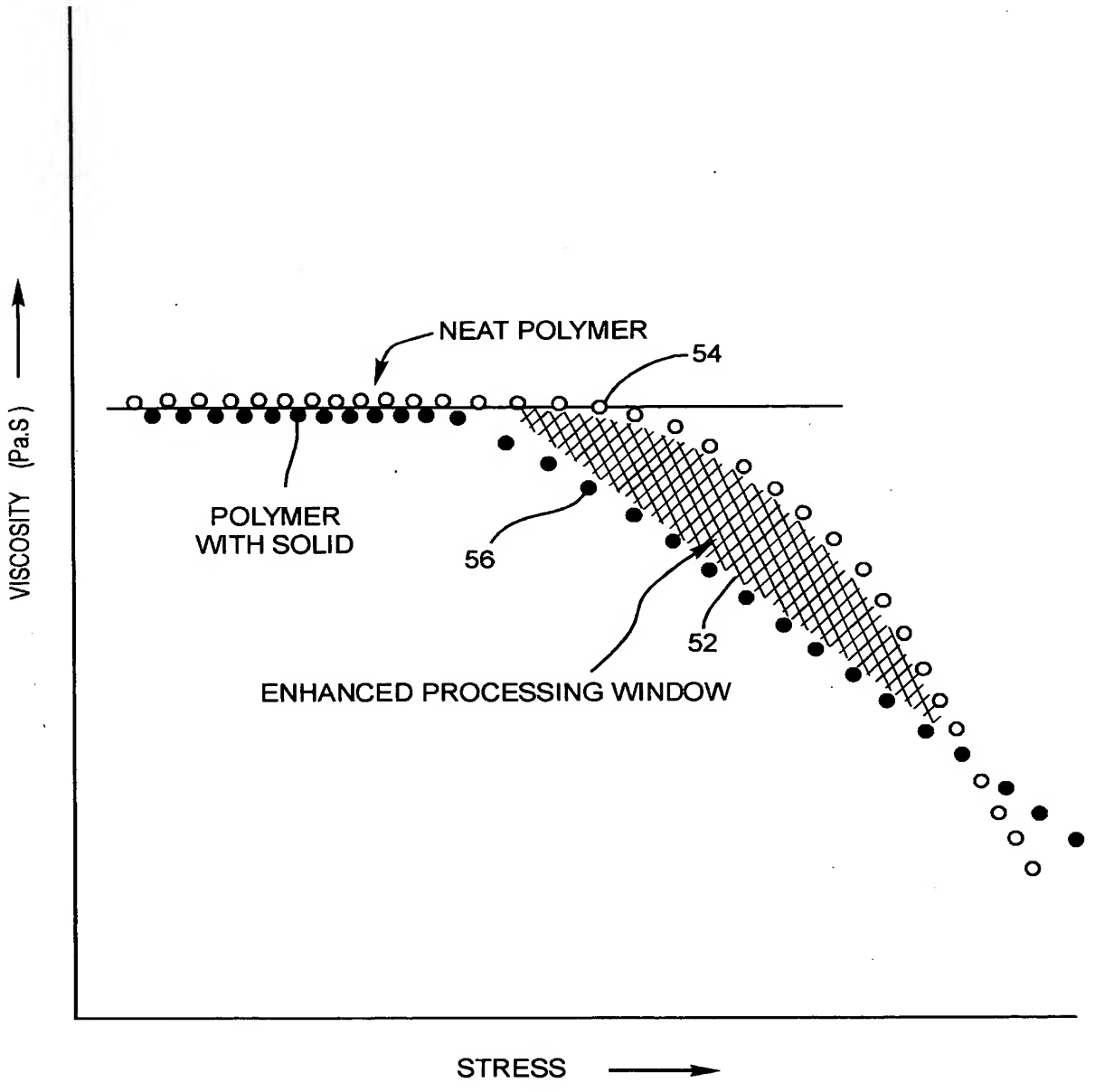

Fig. 7

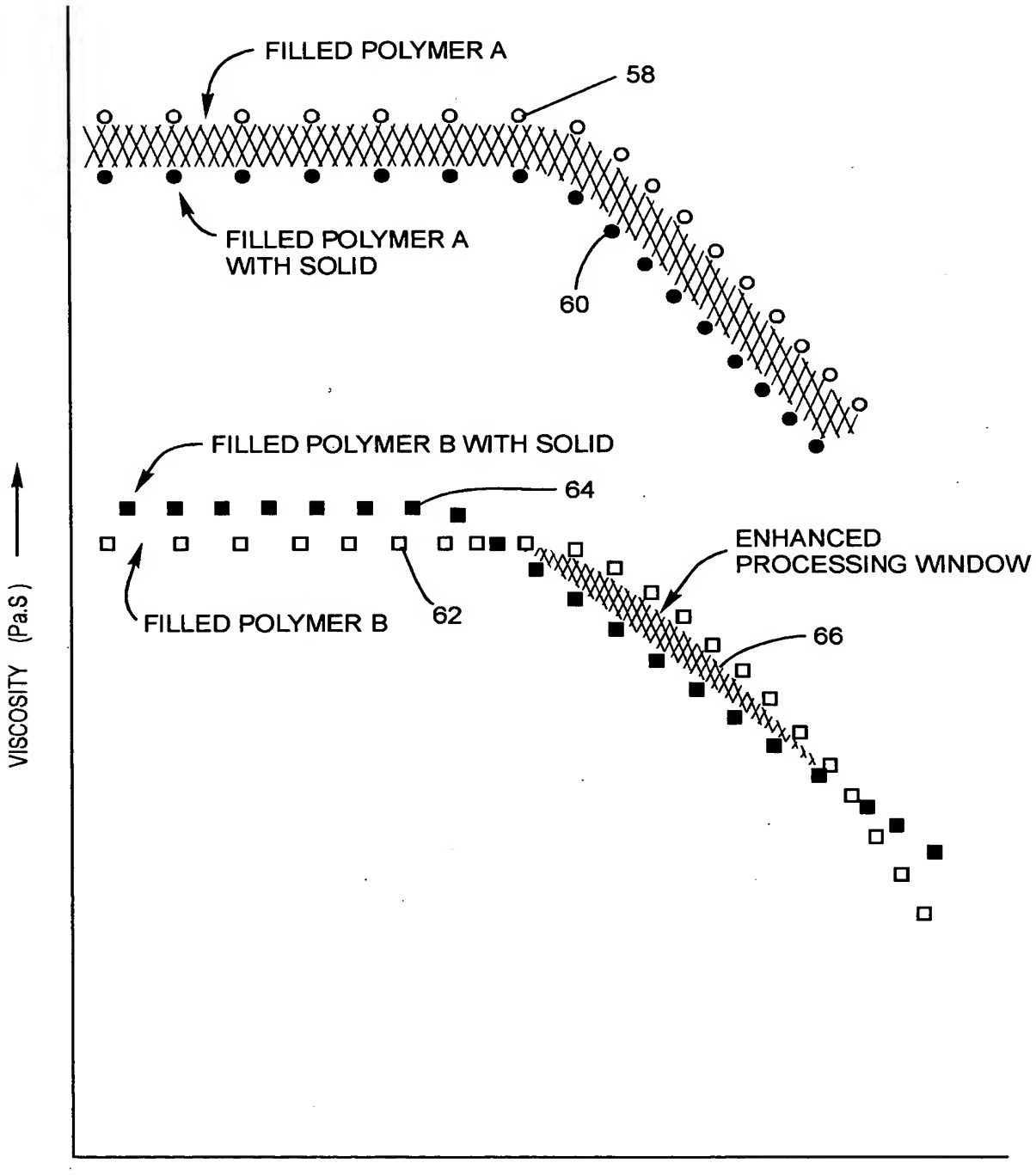

PROCESSING WINDOW OF FILLED POLYMERS

Fig. 8

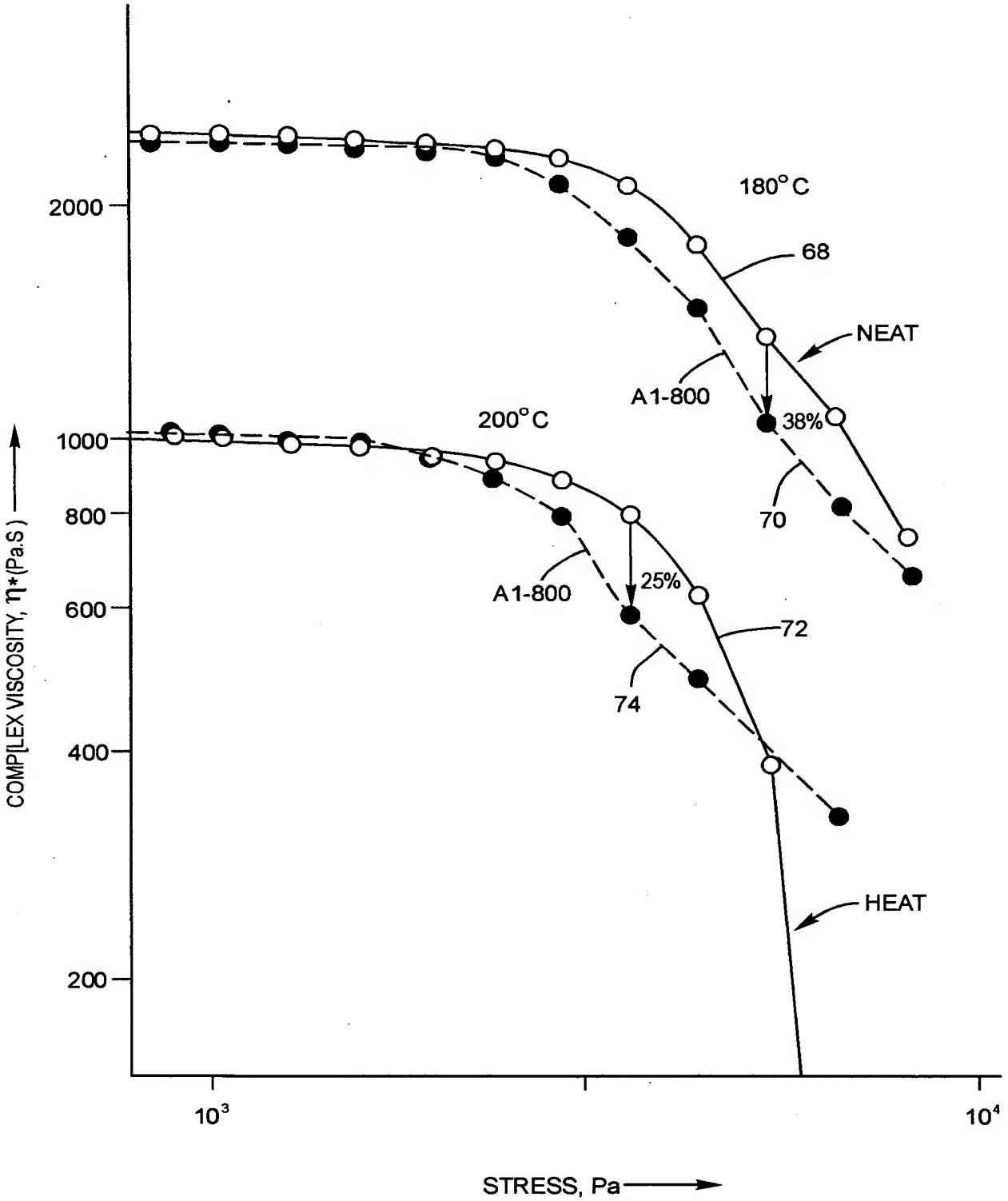

COMPLEX VISCOSITY OF AMORPHONS SOLID A1-800 AND NEAT PP

Fig. 9

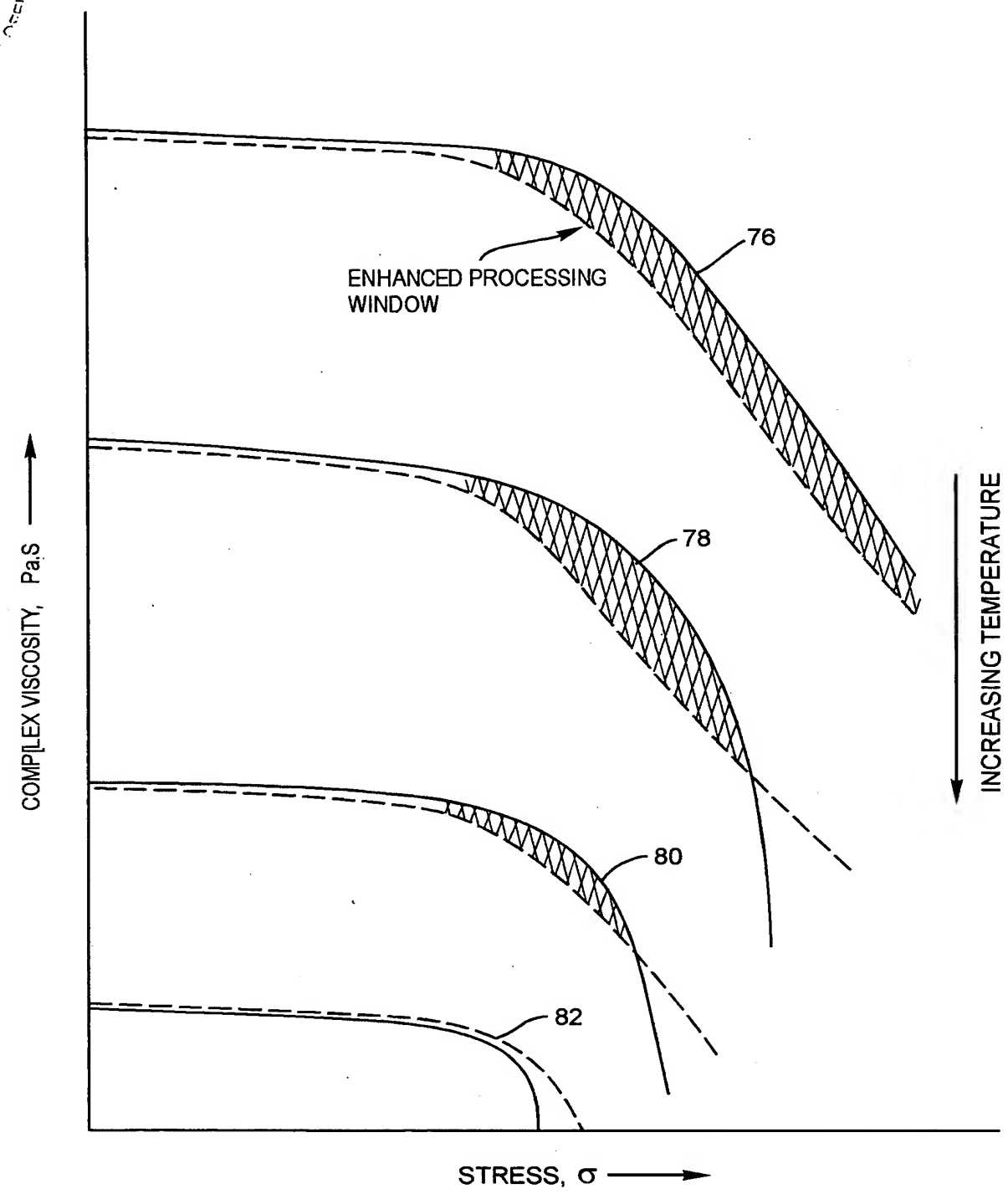

EFFECT OF INCREASING TEMPERATURE ON ENHANCED PROCESSING WINDOW

Fig. 10

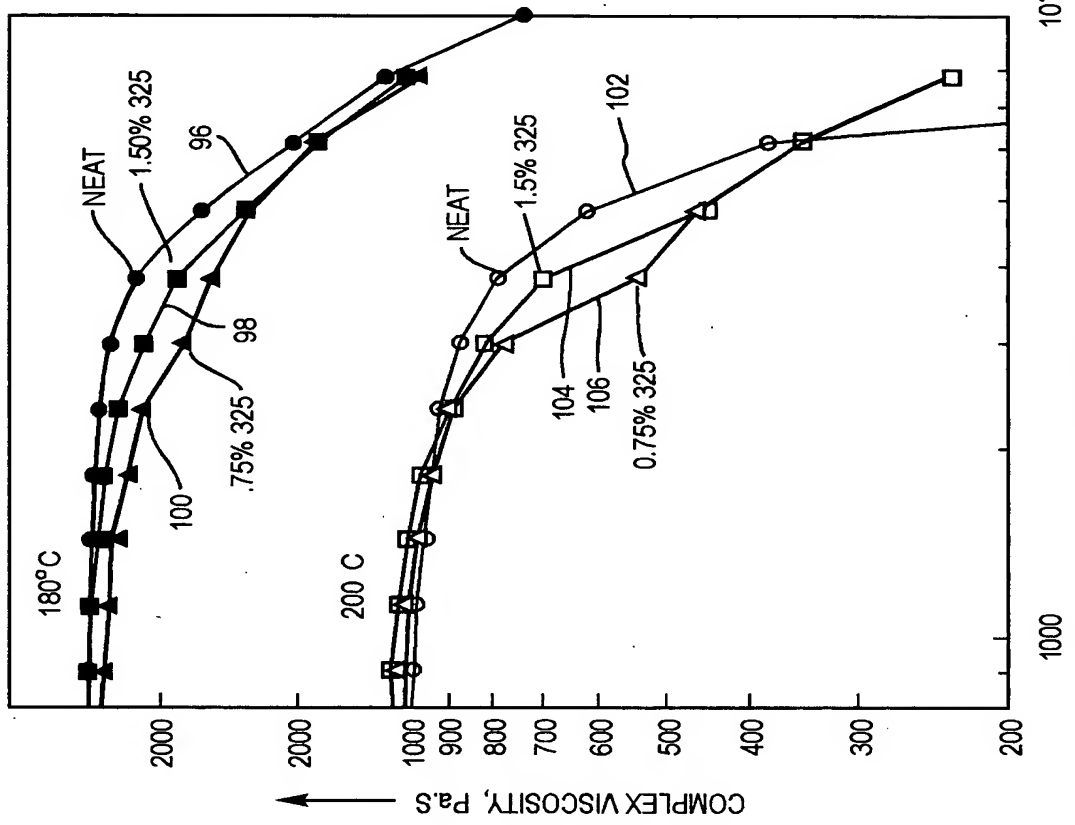

Fig. 11B

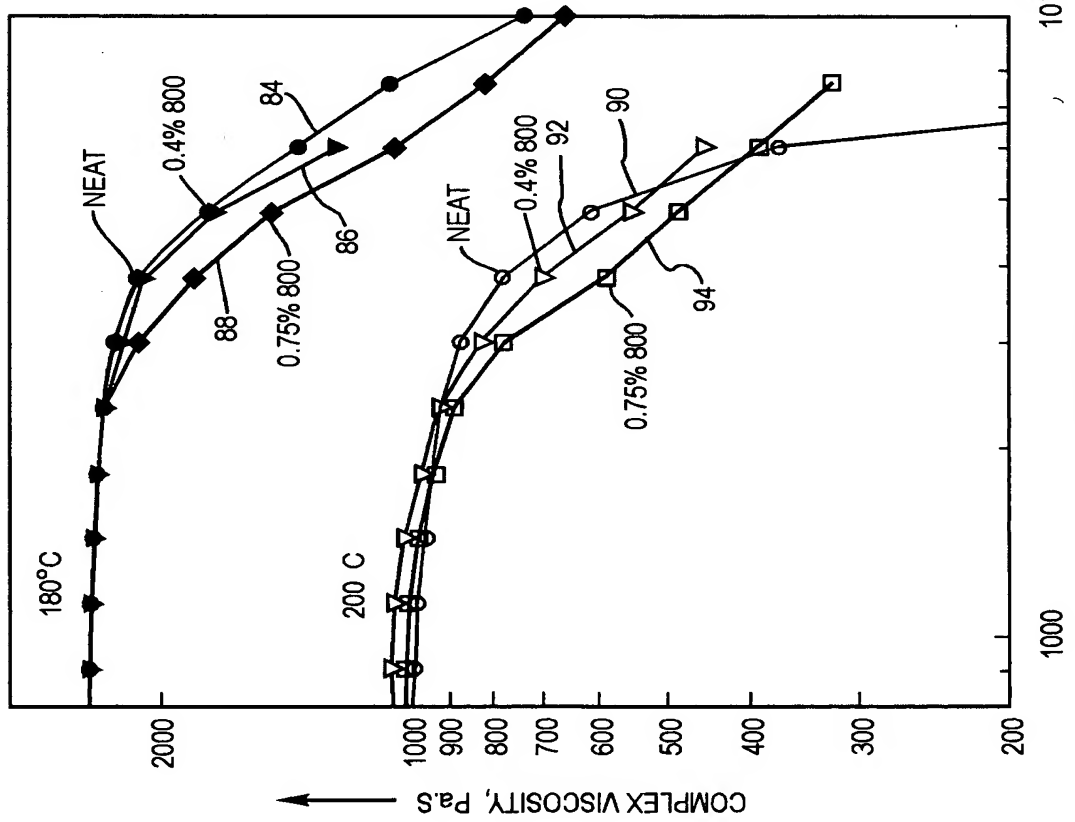

Fig. 11A

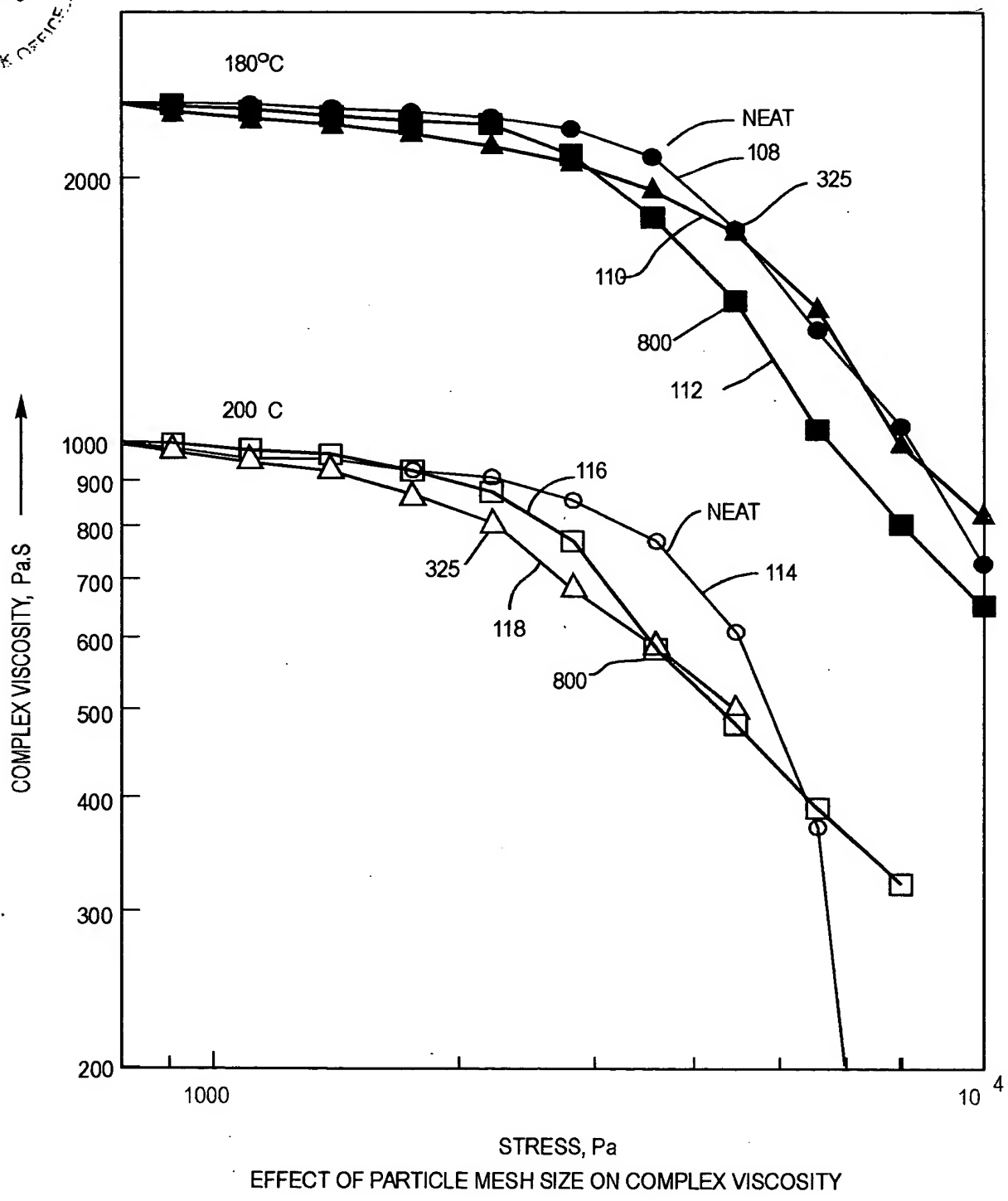

EFFECT OF PARTICLE MESH SIZE ON COMPLEX VISCOSITY

Fig. 12

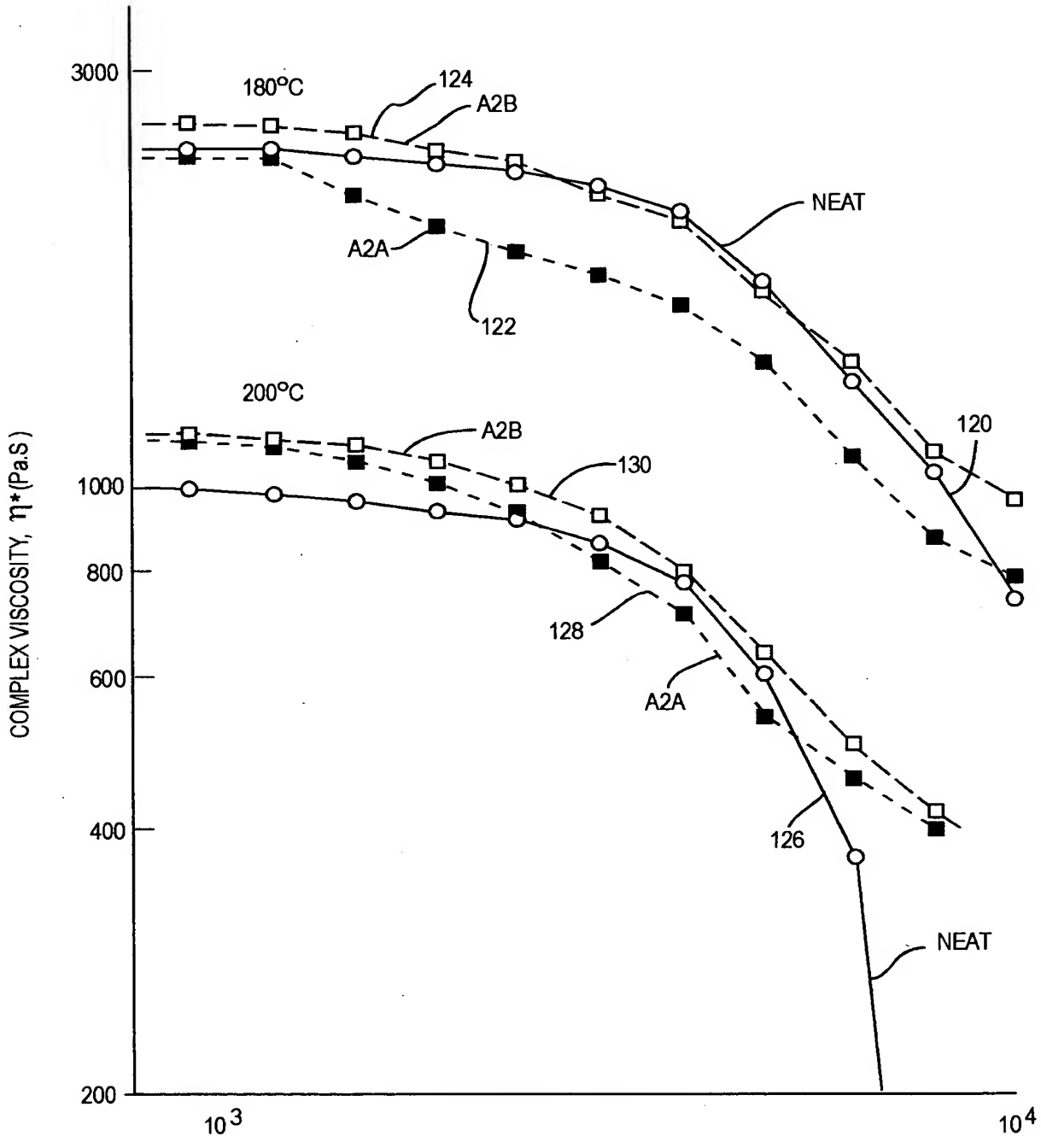

COMPLEX VISCOSITY OF 800-MESH AMORPHOUS SOLID A2 WITH DIFFERENT PARTICLE SHAPES

Fig. 13

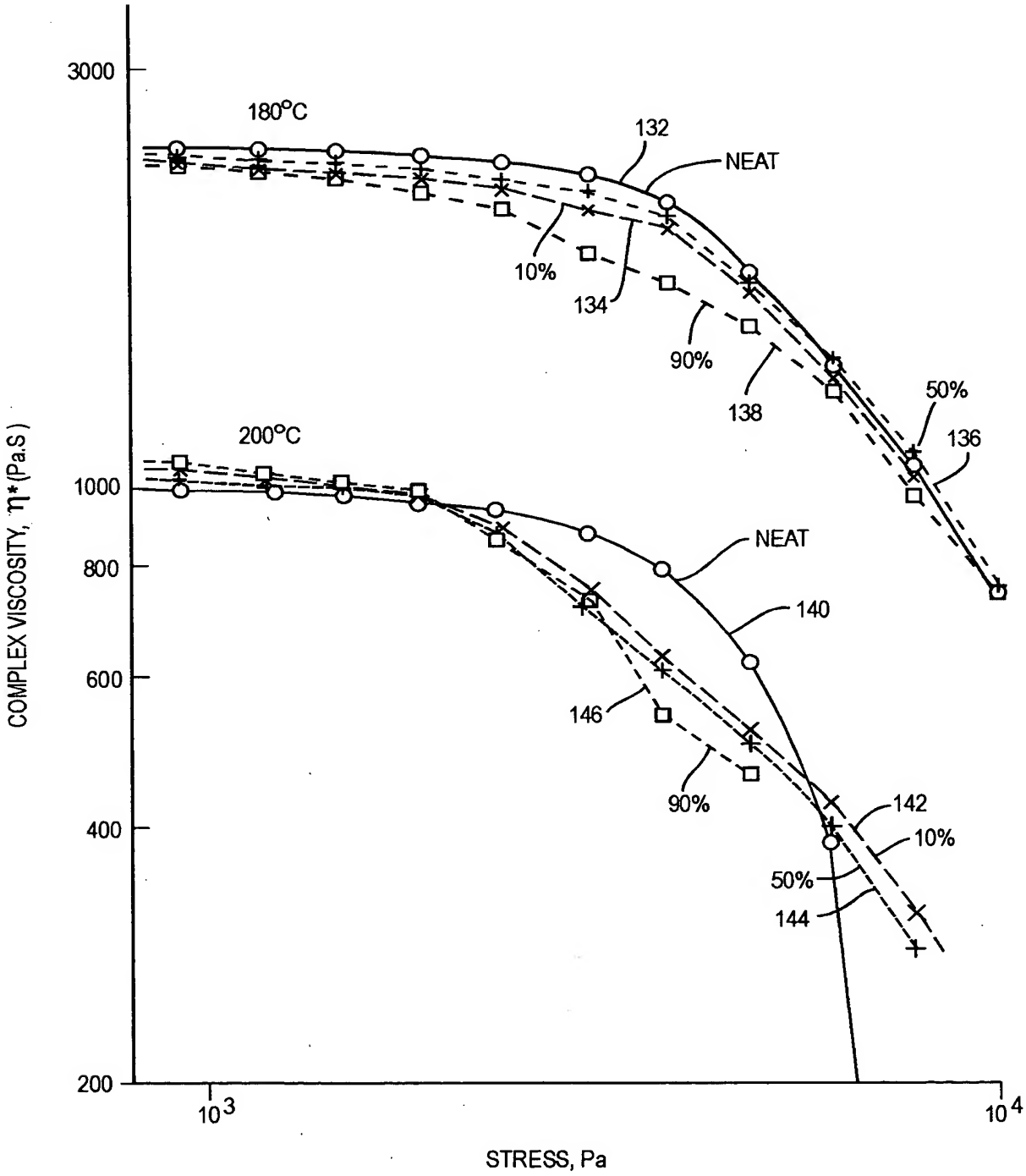

EFFECT OF GLASS CONTENT ON COMPLEX VISICOSITY

Fig. 14

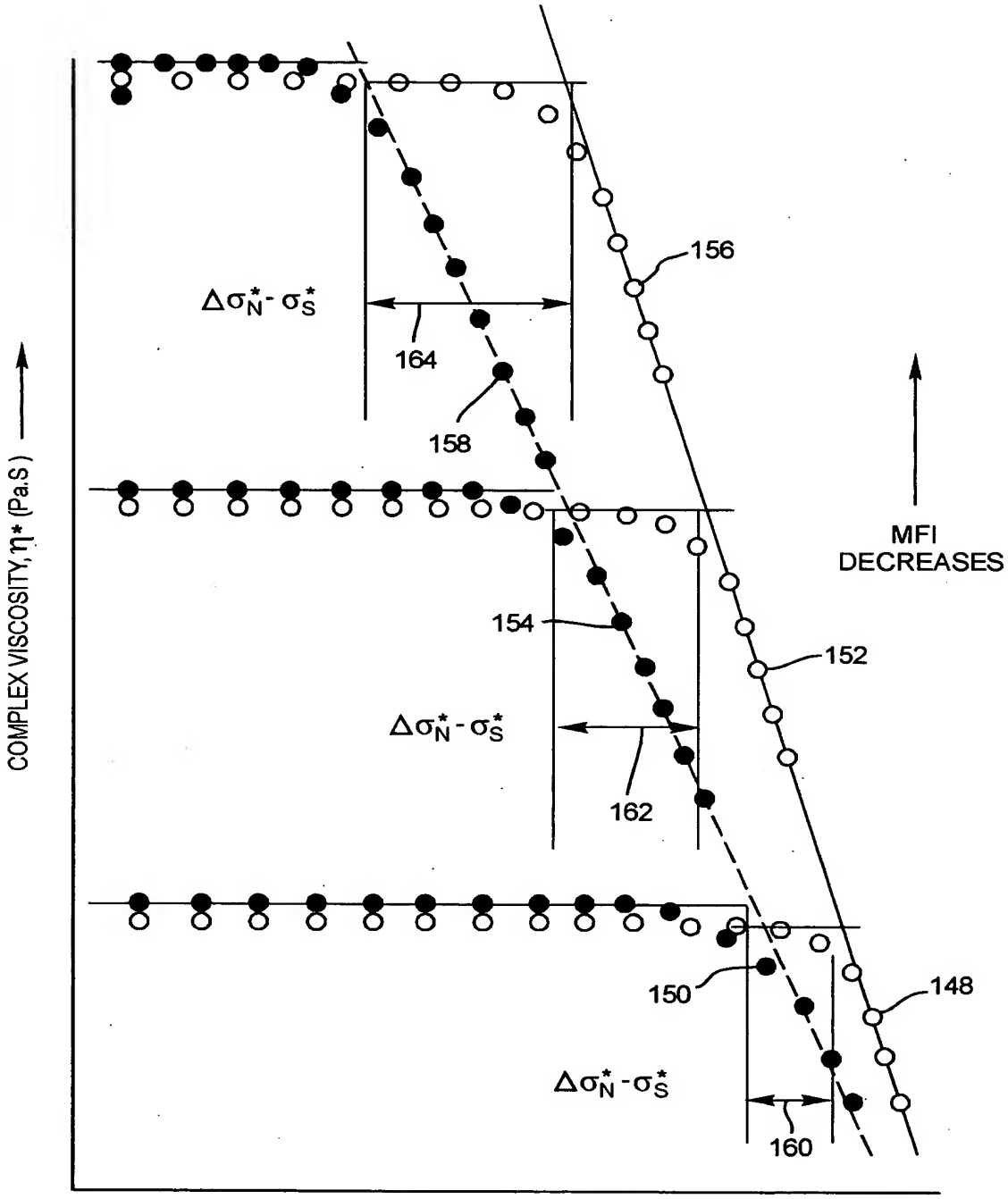

VARIATION IN $\Delta\sigma_N^*$ σ_S^* AS A FUNCTION OF INCREASING MFI FOR A GIVEN POLYMER TYPE

Fig. 15

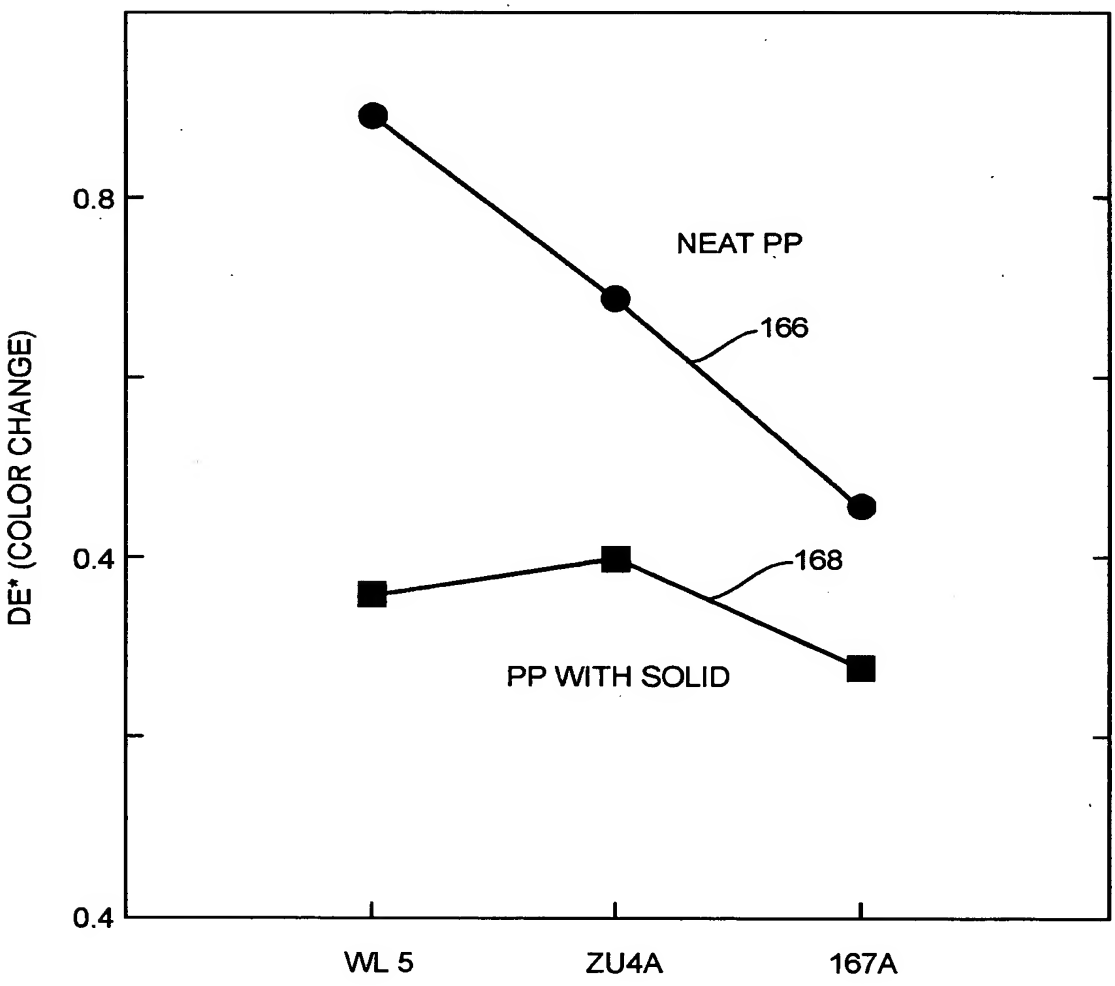

COLOR CHANGE (dE*) IN POLYPROPYLENE AFTER UV LIGHT EXPOSURE

Fig. 16

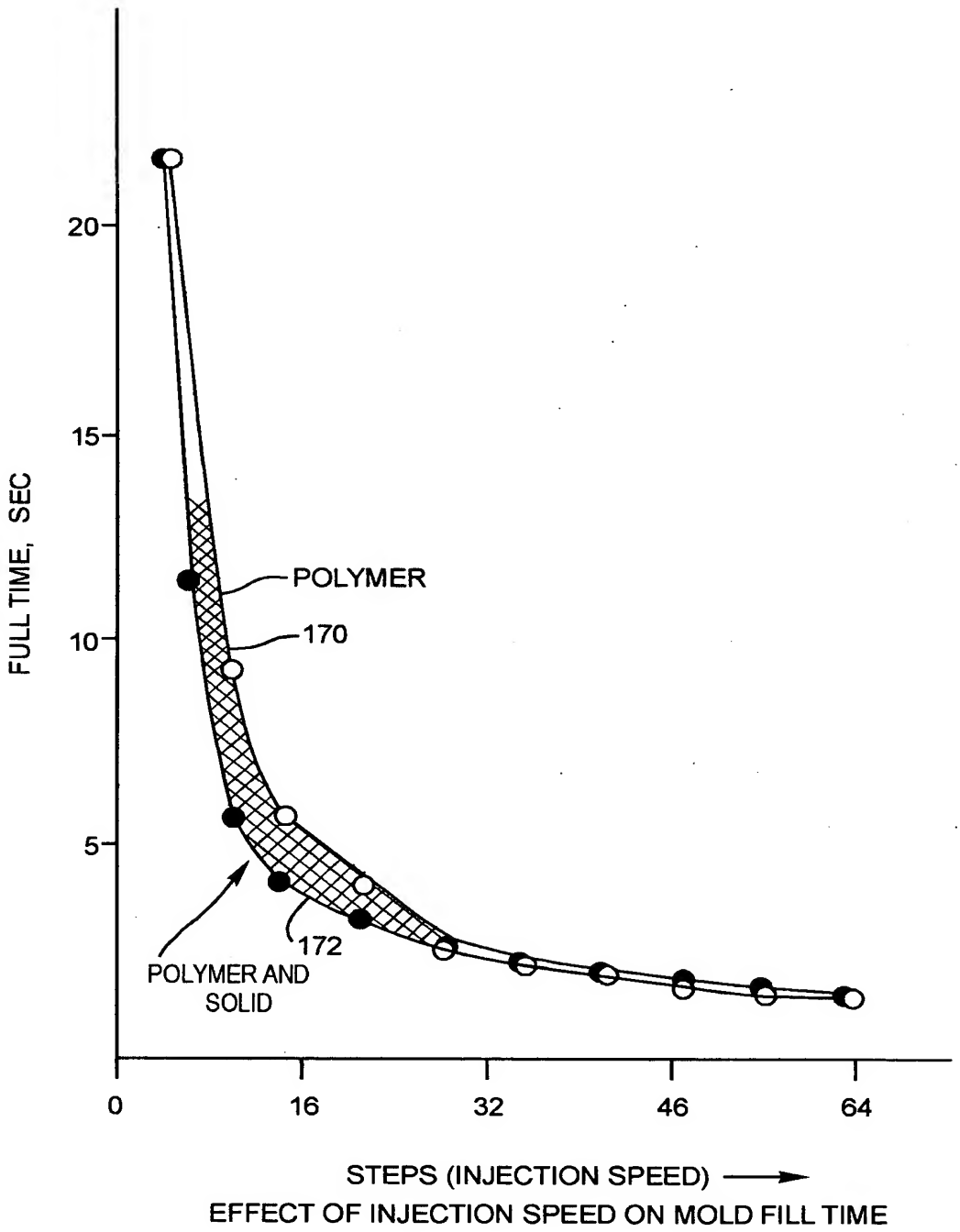

Fig. 17

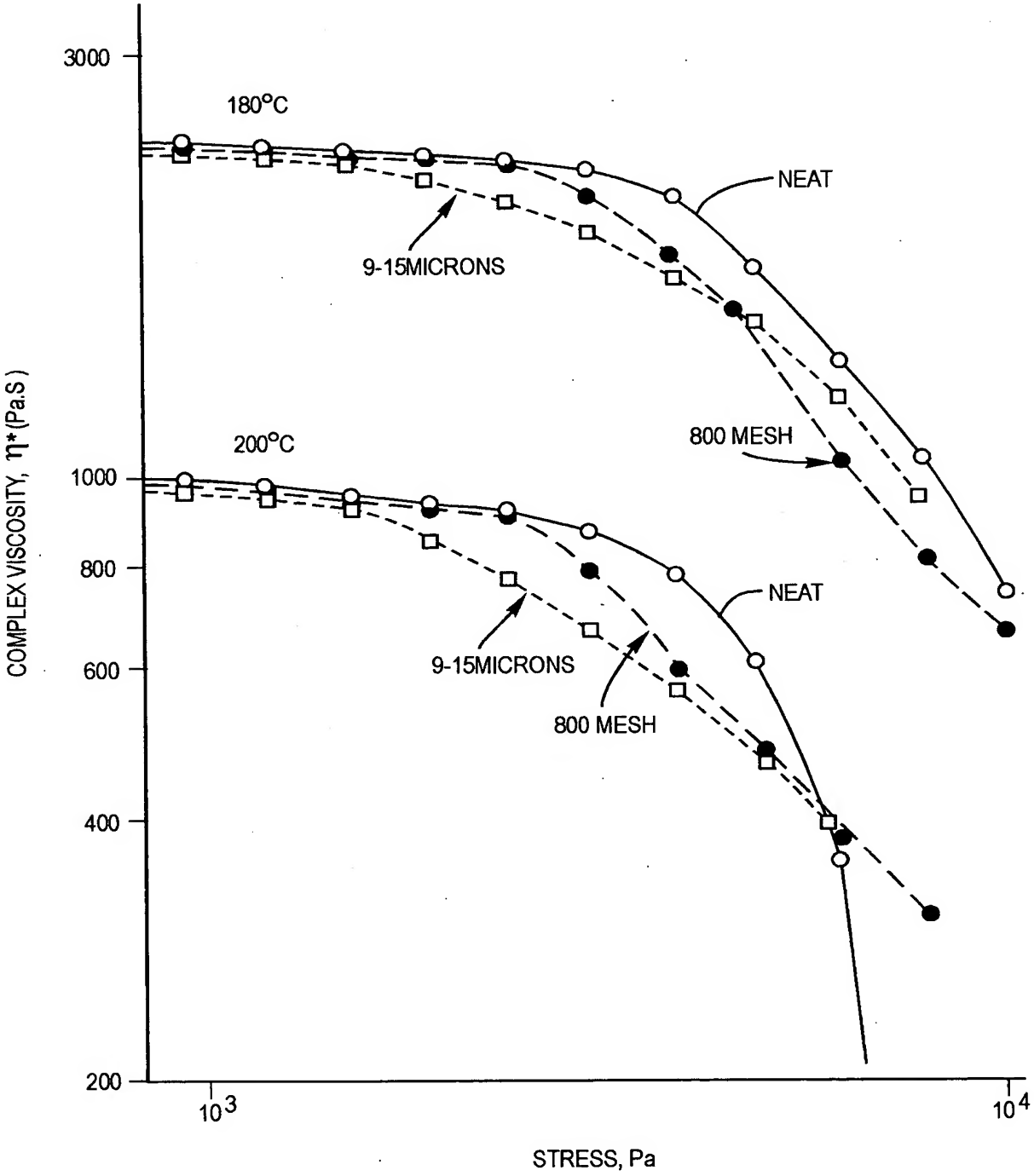

VISCOSITY OF 800-MESH AMORPHOUS SOLID A1 AS COMPARED TO AMORPHOUS SOLID A1 CLASSIFIED TO 9-15 MICRONS

Fig. 18

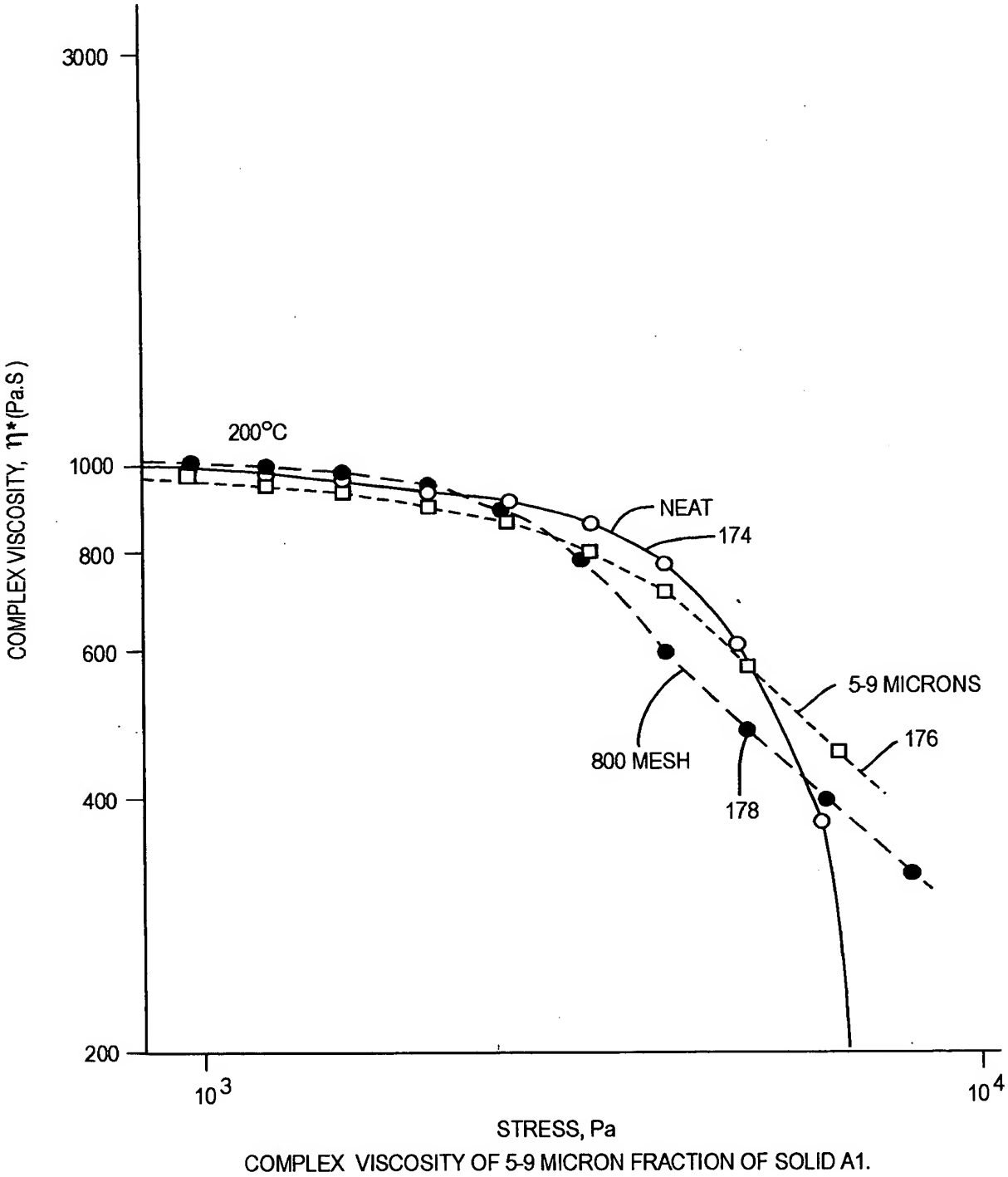

COMPLEX VISCOSITY OF 5-9 MICRON FRACTION OF SOLID A1.

Fig. 19

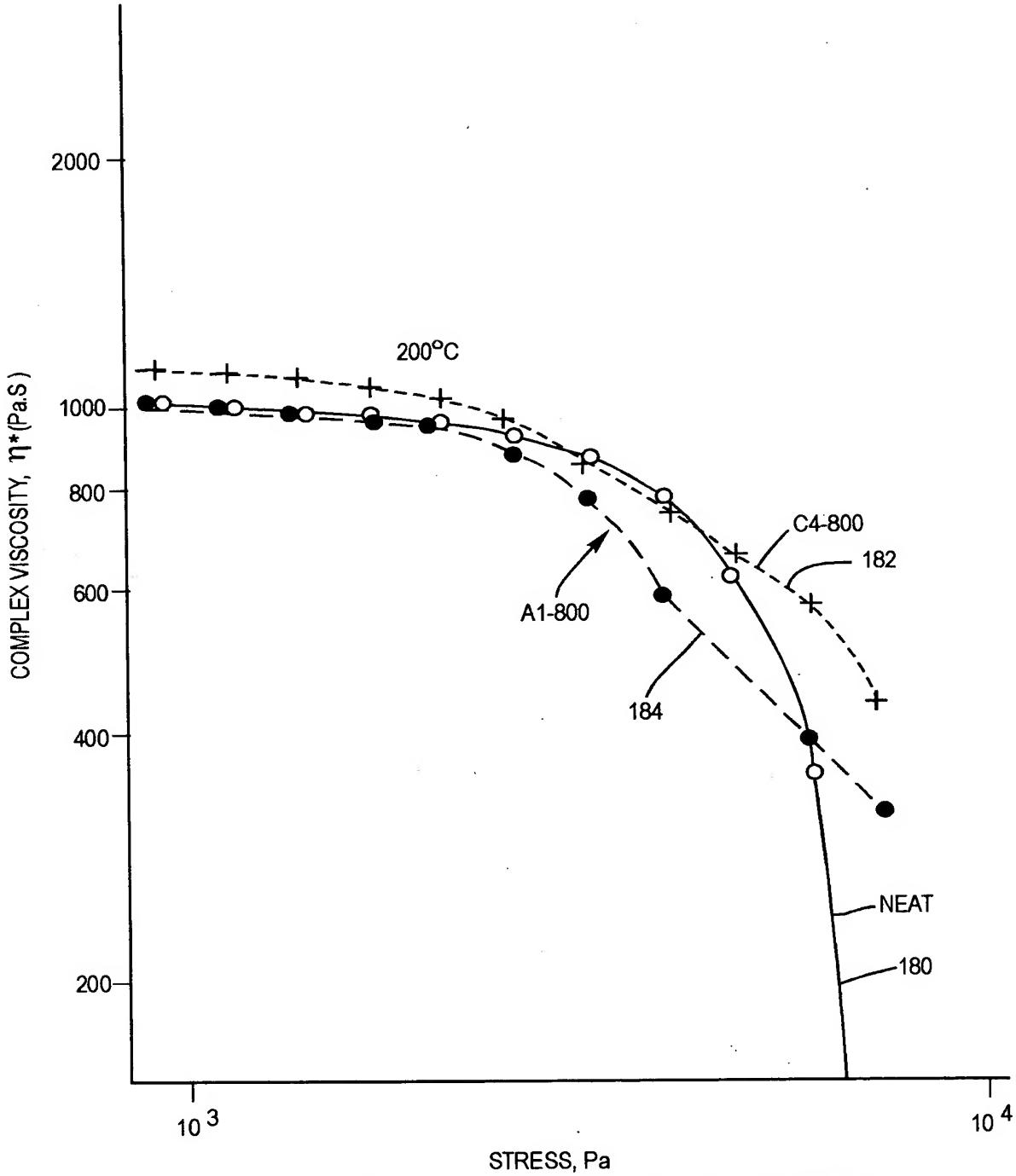

COMPLEX VISCOSITY OF AMORPHOUS MATERIAL, A1-800 MESH, CRYSTALLINE MATERIAL C4-800 MESH AND NEAT PP

Fig. 20

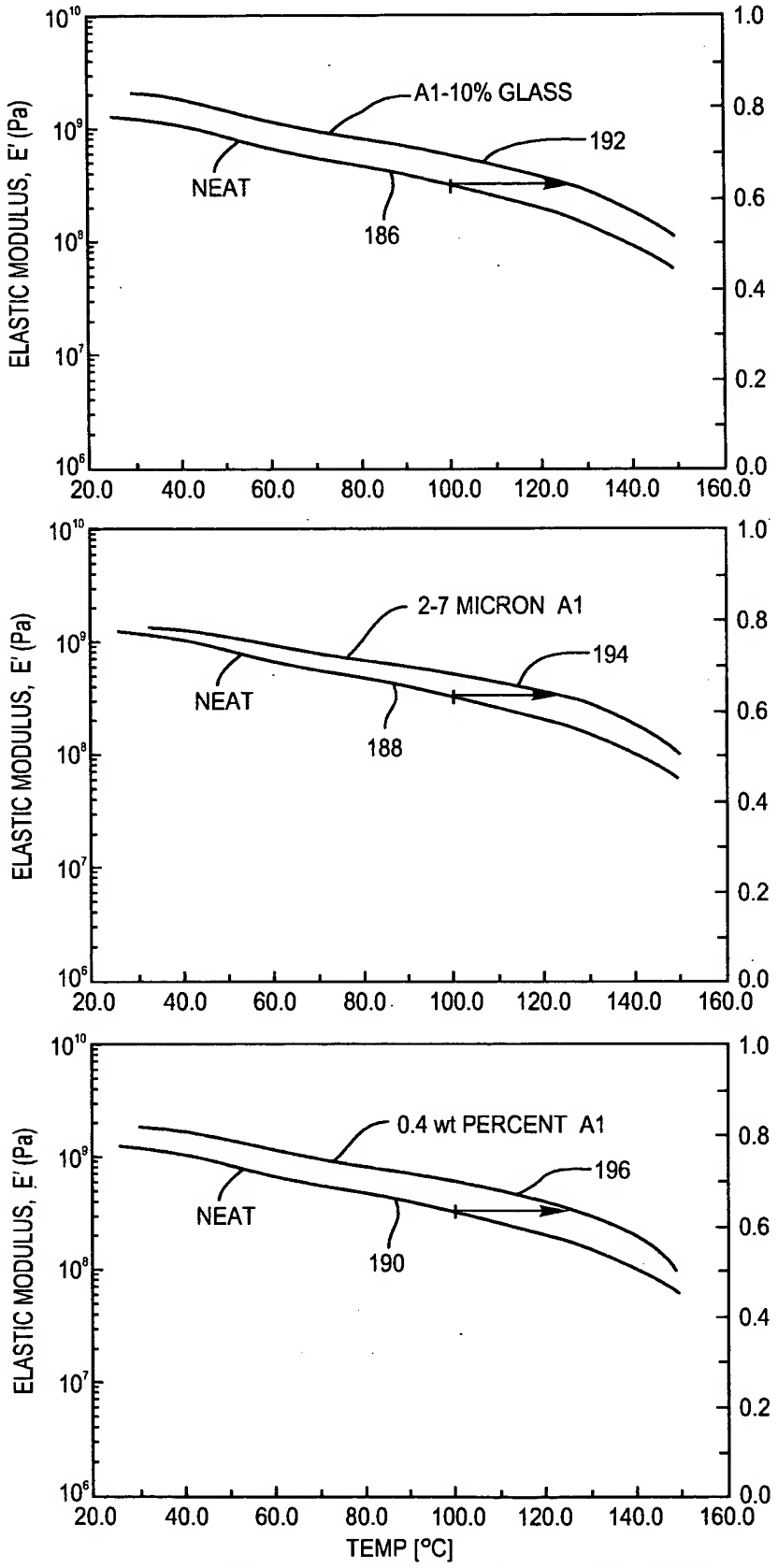

Fig. 21 EFFECT OF PARTICLE CHARACTERISTICS ON DYNAMIC TENSILE ELASTIC MODULUS.